Journal of Integrative Neuroscience

J. Integr. Neurosci. **2025**; 24(8): 39897
https://doi.org/10.31083/JIN39897

Original Research

Remote Ischemic Conditioning Attenuates Apoptosis, the Inflammatory Response, and Reperfusion Injury in Ischemic-Stroke Model Rats via the ELA-Apelin-APJ System

Feng Zhou[1,†], Yangyang Wu[1,†], Xuan Chen[1], Zhuoli Pan[1], Xiaolong Wang[1], Shengwei Gao[1], Chenle Shi[1], Jie Ren[2], Jing Shi[1,*]

[1]Department of Neurology, Peking University First Hospital Taiyuan Hospital, 030000 Taiyuan, Shanxi, China
[2]Department of Dermatology, Peking University First Hospital Taiyuan Hospital, 030000 Taiyuan, Shanxi, China
*Correspondence: 43648931@qq.com (Jing Shi)
[†]These authors contributed equally.
Academic Editor: Hahn Young Kim
Submitted: 22 April 2025 Revised: 18 July 2025 Accepted: 28 July 2025 Published: 28 August 2025

Abstract

Background: Remote ischemic conditioning (RIC), a novel neuroprotective therapy, has broad potential for reducing the occurrence and recurrence of cerebrovascular events, yet its mechanisms are not incompletely understood. The aim of this study is to investigate whether RIC alleviates apoptosis, inflammation, and reperfusion injury in rat models of ischemic stroke by regulating the Elabela (ELA)-apelin-Apelin receptor (APJ) system. **Methods**: We established a rat model of middle cerebral artery occlusion (MCAO) with ischemia-reperfusion injury, and RIC was administered twice daily for 3 days post-MCAO. Cerebral infarct volume was measured and neuronal damage was assessed. Apoptosis-related caspase-3 expression was detected by Terminal deoxynucleotidyl Utransferase nick-End Labeling (TUNEL) and Western blotting (WB). WB was also used to measure apelin, signal transducer and activator of transcription 3 (STAT3), and p-STAT3 protein levels in infarcted brain tissue. ELA miRNA expression was evaluated. Immunofluorescence was used to detect hypoxia-inducible factor 1α (HIF-1α) and activating transcription factor 4 (ATF4) expression. Serum levels of tumor necrosis factor-α (TNF-α) and interleukin-1β (IL-1β) were measured using enzyme-linked immunosorbent assay (ELISA). **Results**: RIC reduced the cerebral infarct volume and neuronal damage in MCAO rats. Compared with the MCAO group, the RIC-treated group (MCAO+RIC) presented significantly lower caspase-3, TNF-α, IL-1β, p-STAT3, HIF-1α, and ATF4 expression ($p < 0.05$), whereas STAT3 and ELA miRNA expression and apelin protein levels were increased ($p < 0.05$). While positively correlated with STAT3 expression, Elabela and apelin levels exhibited a negative correlation with caspase-3 ($p < 0.05$). **Conclusions**: RIC mitigates MCAO-induced neuronal apoptosis, inflammation, and reperfusion injury by modulating the ELA-apelin-APJ system, highlighting its therapeutic potential for ischemic stroke.

Keywords: ischemic stroke; apelin; apoptosis; inflammatory respond; reperfusion injury; middle cerebral artery occlusion

1. Introduction

Data from the 2019 Global Burden of Disease report indicate that stroke persists as a major global health burden, ranking as the world's second most common cause of mortality (accounting for 11.6% of all deaths) and the third primary contributor to combined death and disability (representing 5.7% of total disability-adjusted life years (DALYs) [1]. Large vessel occlusion (LVO) accounts for 15–30% of ischemic strokes and demonstrates disproportionately elevated morbidity and mortality burdens relative to other ischemic stroke subtypes [2]. Despite constituting the established standard of care for LVO-induced acute ischemic stroke, endovascular thrombectomy (EVT) is associated with death or permanent disability in approximately 50% of successfully reperfused patients [3,4]. Improving post-EVT outcomes remains a critical clinical challenge.

Remote ischemic conditioning (RIC) entails applying transient ischemia-reperfusion cycles to distant tissues, conferring protection against subsequent prolonged ischemic insults in remote organs. A study has confirmed that RIC reduces stroke recurrence and improves patient prognosis [5]. Research has demonstrated that RIC exerts neuroprotective effects against cerebral ischemia-reperfusion injury, with these effects occurring in two distinct phases: an early phase (within 24 h after remote ischemic preconditioning) and a late phase (lasting up to 7 days or even 2 months after preconditioning) [6]. As a neuroprotective strategy, RIC has been explored in vascular recanalization therapies. The RIC-cerebral circulation time (CCT) trial demonstrated that short-term RIC significantly improved cerebral circulation time on the stenotic side, reduced contrast medium leakage, and lowered the incidence of cerebral hyperperfusion syndrome after carotid artery stenting in patients with severe internal carotid artery stenosis [7]. Nevertheless,

the neuroprotective pathways of RIC during vascular recanalization are not fully elucidated.

The apelinergic system comprises apelin and Elabela (ELA) peptidergic ligands signaling through their cognate receptor Apelin receptor (APJ), a G protein-coupled receptor [8]. Apelin demonstrates selective neuroanatomical localization within the thalamus, frontal cortex, and hippocampus, modulated by key transcriptional regulators, including hypoxia-inducible factor 1α (HIF-1α), signal transducer and activator of transcription 3 (STAT3), and activating transcription factor 4 (ATF4) [9–11]. Post-stroke neuronal injury results from interconnected pathological processes, including the induction of neuronal apoptosis, activation of the inflammatory cascade, disruption of immune homeostasis, and breakdown of the blood-brain barrier. Cerebral ischemia induces apoptotic programmed cell death, mediated through homeostatic balance between proapoptotic and antiapoptotic genetic pathways [12]. The apelinergic system critically mediates poststroke functional recovery through attenuation of neuronal apoptosis and neuroinflammation. Under hypoxic conditions, apelin/APJ expression is upregulated, potentially mediated by HIF-1α, which binds to hypoxia-response elements (HREs) in the promoter regions of *apelin/APJ* genes, driving their transcriptional activation [13]. In murine models of ischemic stroke, apelin-13 suppresses proinflammatory cytokine transcription, significantly reducing tumor necrosis factor-α (*TNF-*α) and interleukin-1β (*IL-1*β) mRNA levels. Apelin-13 treatment increases apelin/APJ and B-cell lymphoma 2 (Bcl-2) levels while reducing the activation of caspase-3, a key apoptosis-related gene, thereby enhancing cerebral blood flow restoration and promoting sustained functional recovery [14]. ELA, which is expressed predominantly in neurons surrounding cerebral infarct areas, suppresses ischemia-reperfusion (I/R)-induced ferroptosis and lipid peroxidation, mitigating infarct volume and neuronal degeneration [15]. Exogenous ELA administration has also been shown to alleviate direct neurotoxic effects under oxygen-glucose deprivation conditions [16]. In middle cerebral artery occlusion (MCAO) models, cerebrovascular endothelial cells exhibit marked increases in ELA and APJ expression. The ELA-APJ axis enhances angiogenic activity via the Yes-associated protein/transcriptional coactivator with Post-synaptic density protein (PSD95), Drosophila disc large tumor suppressor (Dlg1), Zonula occludens-1 (ZO-1) binding motif (PDZ-binding motif) (YAP/TAZ) pathway, promoting neovascularization and cerebral perfusion recovery and ultimately attenuating I/R injury [17]. Those findings collectively underscore the neuroprotective role of the apelinergic system in cerebral I/R injury. However, whether RIC, an emerging therapeutic intervention, mitigates apoptosis, inflammation, and reperfusion injury in ischemic stroke by modulating the apelinergic system, remains unexplored. In the present study, therefore, we hypothesizes that RIC reduces apoptosis, inflammatory responses, and reperfusion damage in MCAO rats through the regulation of the apelinergic system (Fig. 1). To test this hypothesis, we measured the cerebral levels of apelin, ELA, caspase-3, HIF-1α, ATF4, STAT3, TNF-α, and IL-1β in MCAO rats to validate the neuroprotective mechanisms of RIC.

2. Materials and Methods

2.1 Grouping

Male Sprague-Dawley (SD) rats (n = 27) were randomized into three groups (n = 9/group): Sham-operated controls, MCAO model, MCAO+RIC intervention.

2.2 Animals

Male specific-pathogen-free (SPF) SD rats (6–8 weeks old, 235 $\pm$ 15 g) were purchased from the Experimental Animal Center, Beijing Huafukang Biotechnology Joint Stock Co., Ltd. SCXK (Beijing) 2019-0008. Following a 7-day acclimation period with ad libitum access to standard chow and tap water, animals were maintained under controlled conditions: 20–26 °C ambient temperature, 40%–70% humidity, and 12-h light/dark cycles. Throughout the study, diet and water access remained unchanged, with routine sanitation of housing facilities.

Following one week of acclimatization, rats were randomly assigned for MCAO modeling. Animals were anesthetized via intramuscular injection (Sumianxin II (Dunhua Shengda Animal Husbandry Co., Ltd., Dunhua, Jilin, China): 28.57 mg/mL; Zoletil (Virbac S.A., Carros, France): 35.71 mg/mL; 0.2–0.3 mL/kg) and positioned supinely. After standard skin preparation and disinfection, a midline cervical incision exposed the right carotid artery. The external carotid artery was isolated, with proximal ligation of the common and external carotid arteries. Following internal carotid artery clamping, a monofilament was inserted through the common carotid arteriotomy and advanced into the internal carotid artery for 2-hour ischemia induction, followed by 22-hour reperfusion after withdrawal. The MCAO+RIC cohort additionally received remote ischemic conditioning (right femoral artery isolation with 5-min occlusion/5-min release cycles repeated 5 times). Post-procedural assessment included Ludmila Belayev and neurological deficit scoring, with subsequent collection of peripheral blood and brain tissue for analysis.

2.3 Hematoxylin-Eosin (HE) Staining

Following fixation in 4% paraformaldehyde (PFA) (BL-G002, Nanjing Sunbio Biotechnology Co., Ltd., Nanjing, Jiangsu, China) brain tissues were paraffin-embedded, sectioned, and processed for histological analysis. Sections underwent sequential procedures: baking at 60 °C, xylene (33535, Xilong

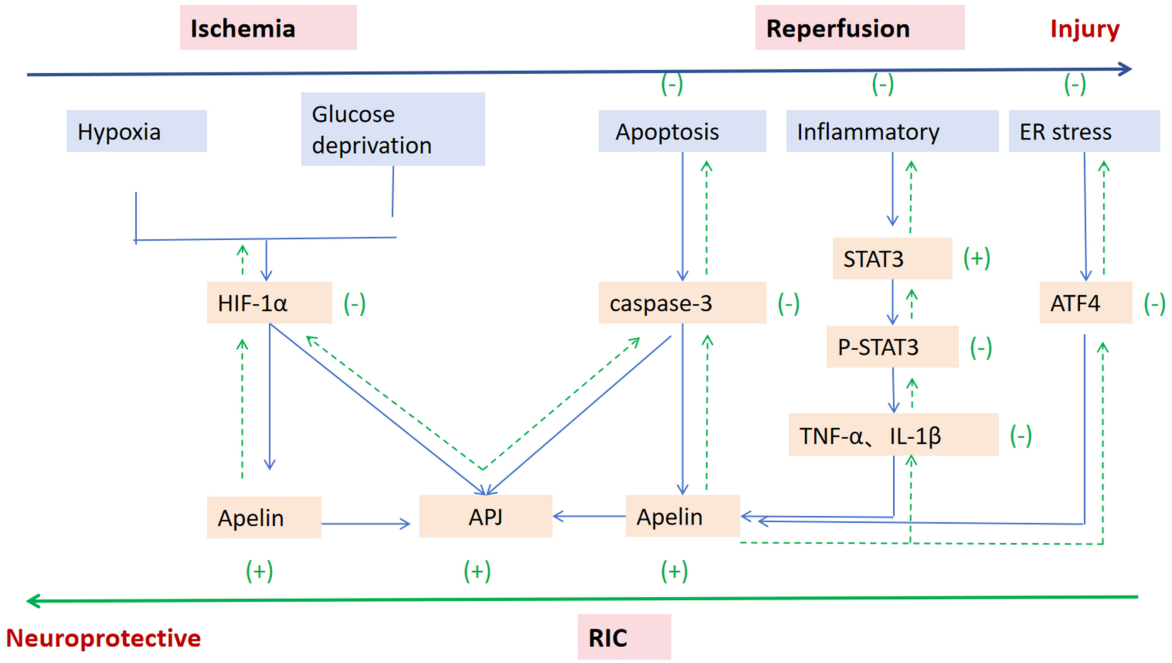

Fig. 1. Schematic of how the ELA-apelin-APJ system mediates RIC neuroprotection (Blue arrows: neuronal damage processes; Green arrows: potential neuroprotective processes elicited by RIC). ELA, Elabela; APJ, apelin receptor; RIC, remote ischemic conditioning; STAT3, signal transducer and activator of transcription 3; HIF-1α, hypoxia-inducible factor 1α; ATF4, activating transcription factor 4; TNF-α,tumor necrosis factor-α; IL-1β, interleukin-1β; ER, endoplasmic reticulum.

Table 1. Primer sequences.

Primer name	Forward primer F (5′-3′)	Reverse primer R (5′-3′)
ELA	CCAGCCCCTTTTTTGGGTATT	TGAAGTGAAATGCATCTCCGG
GAPDH	GACAACTTTGGCATCGTGGA	ATGCAGGGATGATGTTCTGG

GAPDH, Glyceraldehyde-3-Phosphate Dehydrogenase.

Scientific Co., Ltd., Shantou, Guangdong, China) dewaxing, hematoxylin (ZLI-9610, Beijing Zhongshan Jinqiao Biotechnology Co., Ltd., Beijing, China) staining (3–5 min), aqueous rinsing, acid differentiation in 1% hydrochloric acid-alcohol, bluing with 0.2% ammonia water, and eosin (G1100, Beijing Solarbio Scientific Co., Ltd., Beijing, China) counterstaining (3–5 min). After ethanol dehydration and xylene clearance, samples were resin-mounted. Microscopic imaging was performed using an Olympus BX43 (Olympus Corporation, Tokyo, Japan) system with bright-field illumination.

2.4 Enzyme-Linked Immunosorbent Assay (ELISA)

Serum levels of inflammatory mediators IL-1β (E-EL-M0012, Elabscience Biotechnology Co., Ltd.) and TNF-α (E-EL-2856, Elabscience Biotechnology Co., Ltd., Wuhan, Hubei, China) were quantified by ELISA. After centrifugation at 1000 $\times$g (20 min), supernatants were analyzed per manufacturer protocols. Optical density (OD) at 450 nm was determined using a automated microplate reader (WD-2012B, Beijing Liuyi Biotechnology Co., Ltd., Beijing, China).

2.5 Quantitative Polymerase Chain Reaction (qPCR) Assay

ELA gene expression in brain tissue was quantified by qPCR. Total RNA was isolated using TRIzol reagent (CW0580S, Beijing Kinghawk Biotech Co., Ltd., Beijing, China), followed by mRNA purification with an RNA Ultra Pure Extraction Kit (CW0581M, Beijing Kinghawk Biotech Co., Ltd., Beijing, China). cDNA synthesis employed a reverse transcription kit (R223-01, Nanjing Vazyme Biotech Co., Ltd., Nanjing, Jiangsu, China), and amplification performed on a Real-Time PCR System (CFX Connect™, Shanghai Bio-Rad Laboratories Ltd., Shanghai, China) under cycling conditions: 95 °C/30 s (initial denaturation); 40 cycles of 95 °C/10 s, 58 °C/30 s, 72 °C/30 s. Relative expression was normalized to Glyceraldehyde-3-Phosphate Dehydrogenase (*GAPDH*) and calculated via the calculated via the $2^{-\Delta\Delta Ct}$ method. The primer sequences are provided in Table 1.

2.6 Western Blotting (WB)

Protein expression of apelin, STAT3, phosphorylated STAT3 (p-STAT3), and caspase-3 in brain tissue was

analyzed by WB. Briefly, 50 mg tissue samples were homogenized in 1 mL RIPA lysis buffer (C1053, Beijing Applygen Technologies Inc, Beijing, China) using a CryoMill grinder (CryoMill, Retsch GmbH, Haan, Germany) followed by centrifugation at 12,000 rpm (4 °C, 10 min). Supernatants were collected for protein quantification with a BCA assay. After denaturation, proteins underwent SDS-PAGE (1.5 h) and electrophoretic transfer to PVDF membranes (IPVH00010, MilliporeSigma, Burlington, MA, USA). Membranes were blocked with 3% skim milk (RT, 1 h) and probed overnight at 4 °C with primary antibodies: mouse anti-GAPDH (1:2000, HC301, TransGen Biotech, Beijing, China), rabbit anti-apelin (1:1000, df13350, Affinity Biosciences Ltd., Nanjing, Jiangsu, China), anti-STAT3 (1:1000, OM108644, OmniAb, Inc, Emeryville, CA, USA), anti-p-STAT3 (1:1000, bsm-52210R, Bioss Inc, Beijing, China), and anti-caspase-3 (1:1000, A0214, ABclonal Technology, Inc, Wuhan, Hubei, China). After washing, species-matched HRP-conjugated secondary antibodies were applied (goat anti-mouse IgG-HRP, 1:2000, GB23301, Servicebio Technology Co., Ltd., Wuhan, Hubei, China; goat anti-rabbit IgG-HRP, 1:2000, GB23303, Servicebio Technology Co., Ltd., Wuhan, Hubei, China) for 2 h at RT. Protein bands were visualized using ECL substrate (RJ239676, Thermo Fisher Scientific Inc, Shanghai, China) on a fully Automated Chemiluminescence Imaging System (Tanon-5200, Shanghai Tanon Science & Technology Co., Ltd., Shanghai, China).

2.7 Nissl Staining

Paraffin sections underwent sequential processing: baking at 65 °C, deparaffinization in xylene (33535, Xilong Scientific Co., Ltd., Guangdong, China), Nissl staining (G1036, Servicebio Technology Co., Ltd., 5 min), and thorough aqueous rinsing until chromogen clearance. After blot-drying, sections were oven-desiccated ($\geq$4 h at 65 °C) prior to xylene clearing and neutral balsam mounting (YZB, Bio-Thera Solutions, Ltd., Guangdong, China). Histological imaging utilized an Olympus BX43 microscope with bright-field optics.

2.8 Terminal deoxynucleotidyl Utransferase nick-End Labeling (TUNEL) Staining

Tissue sections underwent sequential dehydration/rehydration: ethanol (32061, Xilong Scientific Co., Ltd.) I (3 min), anhydrous ethanol II (3 min), 95% alcohol (3 min), 80% alcohol (3 min), and purified water (2 min). After transfer to a humidified chamber, sections were treated with 50 µg/mL proteinase K (EBY0027J, Cibio Biotech Co., Ltd., Shanghai, China; 37 °C, 30 min), followed by three 5-min Phosphate-Buffered Saline (PBS) washes. Excess PBS was blotted, then TUNEL reaction mixture (C1090, Beyotime Biotechnology Co., Ltd., Shanghai, China) was applied for dark incubation (42 °C, 1 h) with maintained chamber humidity. Post-TUNEL PBS washes preceded 4',6-Diamidino-2-Phenylindole (DAPI) counterstaining (dark, 5 min) and final PBS rinsing. Slides were blotted dry, mounted with antifade medium, and imaged using an Olympus BX53 fluorescence microscope.

2.9 Immunofluorescence Monostaining

Brain sections underwent baking, dewaxing, and hydration followed by citrate-based antigen retrieval. After permeabilization with 0.5% Triton X-100 (RT, 20 min, GC204003, Servicebio Technology Co.) and three 5-min PBS washes, residual buffer was blotted. Sections were blocked with 5% BSA (37 °C, 30 min) prior to overnight incubation at 4 °C with primary antibodies: rabbit anti-HIF-1α (1:200, aF1009, Affinity Biosciences Ltd., Nanjing, Jiangsu, China), anti-GFAP (1:200, DF6040, Affinity Biosciences Ltd.), anti-ATF4 (1:200, 10835-1-AP, Proteintech Group, Inc, Rosemont, IL, USA), and anti-NeuN (1:200, 26975-1-AP, Proteintech Group, Inc). Post-rewarming, slides received three 3-min PBS washes. Cy3-conjugated secondary antibody (1:200, AS007, ABclonal Technology, Inc) was applied for 37 °C incubation in humidified chamber (30 min). Nuclear counterstaining employed DAPI (dark, 3 min) with subsequent PBS rinsing. After tap water wash (1 min), slides were mounted in antifade medium and imaged on an Olympus BX53 fluorescence microscope.

2.10 TTC Staining

After euthanasia via anesthetic overdose (Sumianxin II, 28.57 mg/mL and Zoletil, 35.71 mg/mL, administered via intramuscular injection at a dose of approximately 0.4–0.6 mL/kg), the brains were immediately harvested. Fresh brain samples were placed in a culture dish and flash-frozen at –20 °C for 20–30 min. After partial thawing, the brains were sliced coronally into five evenly spaced sections (2–3 mm thickness per slice). The tissue sections were immersed in pre-warmed (37 °C) 2% 2,3,5-triphenyltetrazolium chloride (TTC, C0652, Beyotime Biotechnology Co., Ltd.) solution and incubated in a 37 °C incubator (temperature strictly maintained below 40 °C) for 30 min under light-protected conditions. During incubation, the tissue was gently agitated every 5 min to ensure uniform staining. Upon color development, the TTC solution was decanted, and tissue was fixed in 4% paraformaldehyde to terminate the reaction and preserve morphology. Images were captured 24 h post-fixation for infarct-volume analysis.

2.11 Statistical Analyses

Statistical analyses employed GraphPad Prism 8.0 (GraphPad Software, LLC, Shanghai, China). Quantitative data are presented as mean $\pm$ SD. Multi-group comparisons used one-way ANOVA with Tukey's post hoc testing. Pearson's correlation assessed variable associations. Significance was defined as two-sided $p < 0.05$.

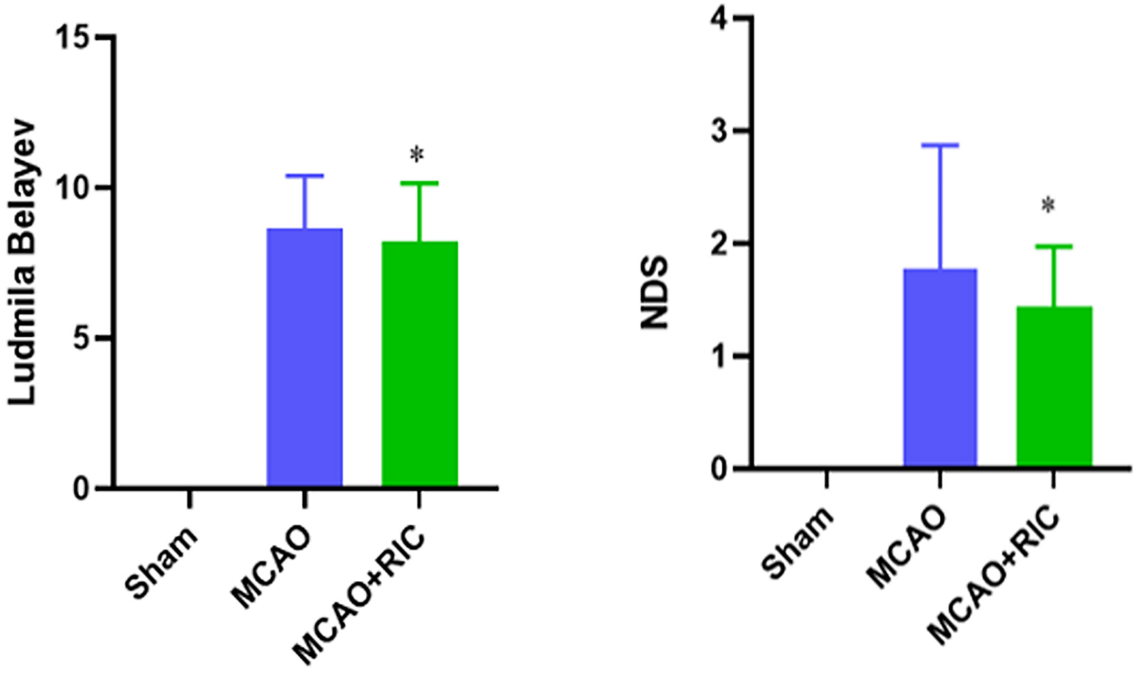

Fig. 2. Ludmila Belayev and NDS scores (*$p < 0.05$ *vs.* the MCAO group). NDS, Neurological Deficit Score; MCAO, middle cerebral artery occlusion.

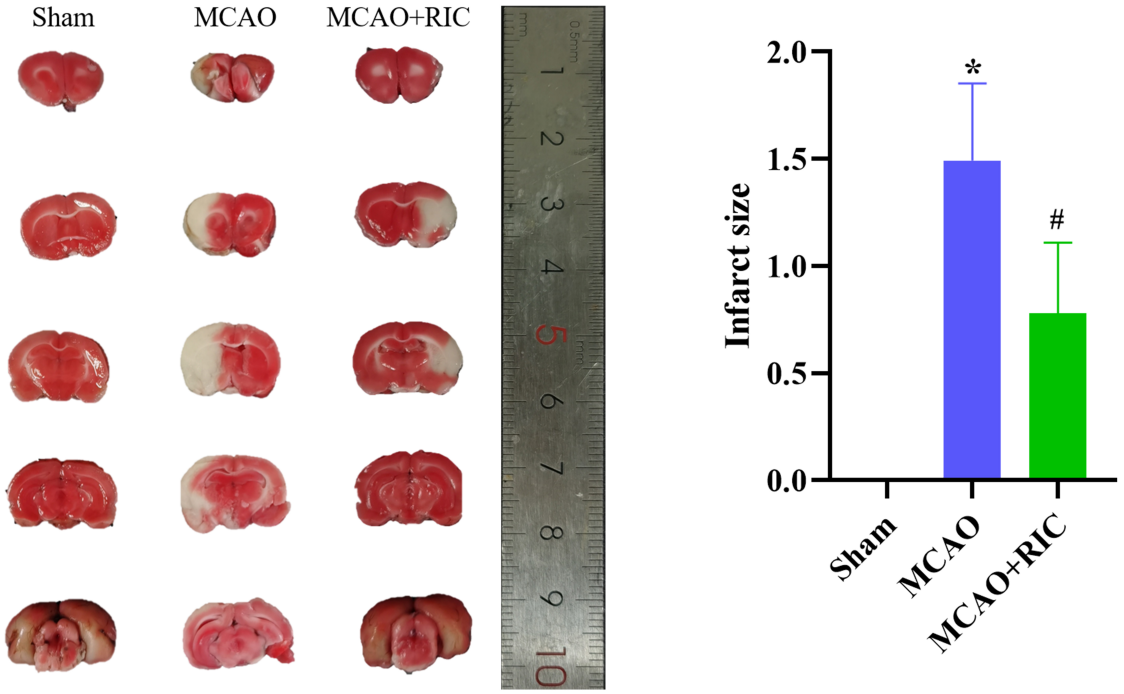

Fig. 3. TTC staining and infarct size: The brain tissues in the sham group presented uniform red coloration, whereas that in the MCAO group presented distinct pale/white regions in the ischemic area. TTC, triphenyltetrazolium chloride.

3. Results

3.1 Behavioral Assessments: Ludmila Belayev Score and Neurological Deficit Score (NDS)

Following 7-day acclimatization, rats were randomized into three cohorts (n = 9/group): sham, MCAO, and MCAO+RIC. Postmodeling behavioral evaluations using the Ludmila Belayev and NDS scales revealed that the MCAO+RIC group presented significantly lower scores than did the MCAO group on both the Ludmila Belayev scale (8.22 ± 1.92 *vs.* 8.67 ± 1.73) and the NDS (1.44 ± 0.53 *vs.* 1.78 ± 1.09) ($p < 0.05$) (Fig. 2).

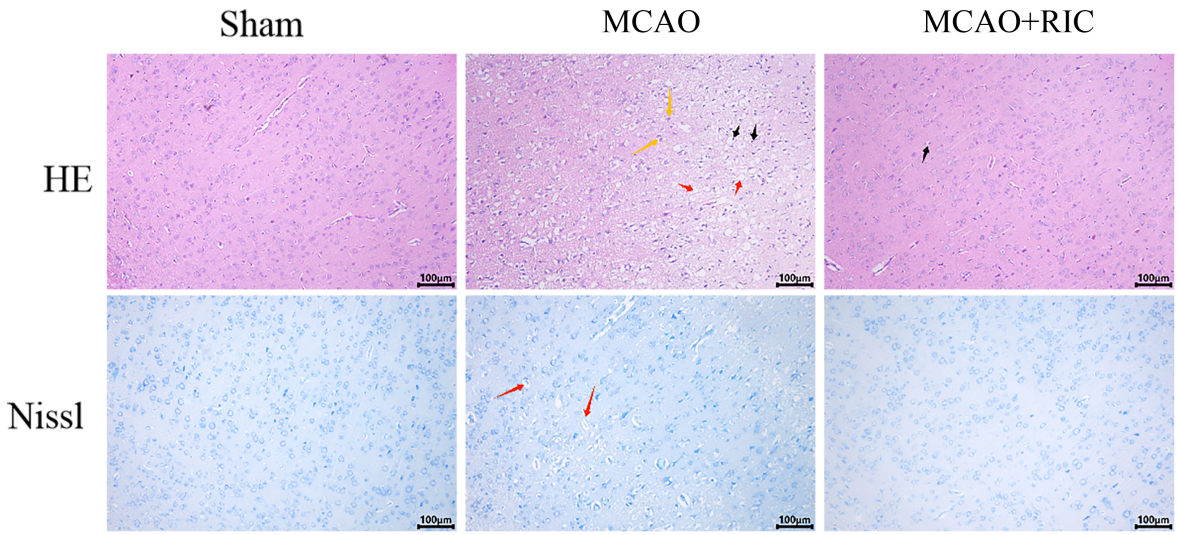

Fig. 4. HE and Nissl staining: shrunken neuronal cells (yellow arrows), nuclear pyknosis and hyperchromasia (black arrows), vacuolar degeneration (red arrows). HE, Hematoxylin-Eosin. The scale bar = 100 μm.

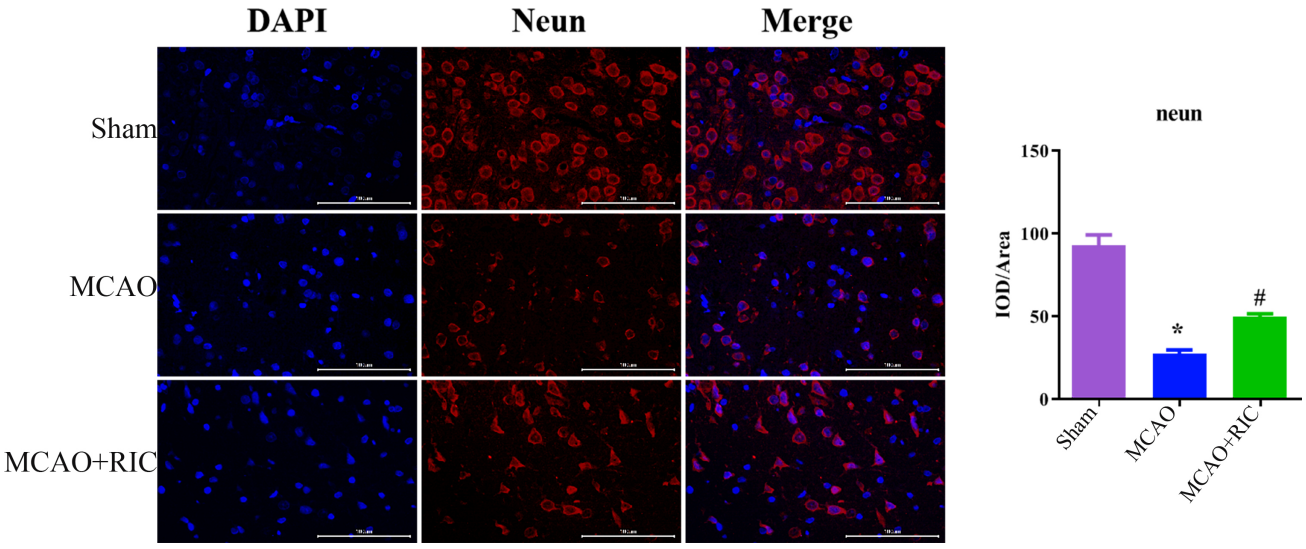

Fig. 5. Immunofluorescence staining (*$p < 0.05$ *vs.* sham; #$p < 0.05$ *vs.* MCAO). The scale bar = 100 μm.

3.2 RIC Reduced the Cerebral Infarct Volume in MCAO Rats

Cerebral infarct areas were assessed via TTC staining across groups (Fig. 3). The brain tissue in the sham group presented uniform red coloration, whereas that in the MCAO group presented distinct pale/white regions in the ischemic area. Compared with the sham group, the MCAO group presented significant necrotic ischemic areas ($p < 0.05$). In contrast, the MCAO+RIC group presented a markedly lower cerebral infarct volume than did the MCAO group ($p < 0.05$).

3.3 RIC Attenuated Neuronal Damage in MCAO Rats

HE staining revealed shrunken neuronal cells (yellow arrows on Fig. 4), widespread nuclear pyknosis and hyperchromasia (black arrows), vacuolar degeneration and necrosis (red arrows) in the cerebral cortex of the MCAO group, indicating severe neuronal injury. In contrast, the MCAO+RIC group exhibited only scattered nuclear pyknosis (black arrows) and markedly reduced neuronal damage. Nissl staining revealed a loss of Nissl bodies, morphological abnormalities, and extensive vacuolation (red arrows) in the cortical neurons of the MCAO group. Conversely, the MCAO+RIC group presented significantly fewer morphological aberrations in Nissl bodies, increased neuronal cell density, and attenuated cortical damage. These findings from HE and Nissl staining collectively indicate that RIC substantially ameliorates neuronal injury (Fig. 4).

Immunofluorescence analysis of NeuN (neuronal nuclear antigen) revealed significantly reduced expression in the MCAO group versus sham controls ($p < 0.05$).

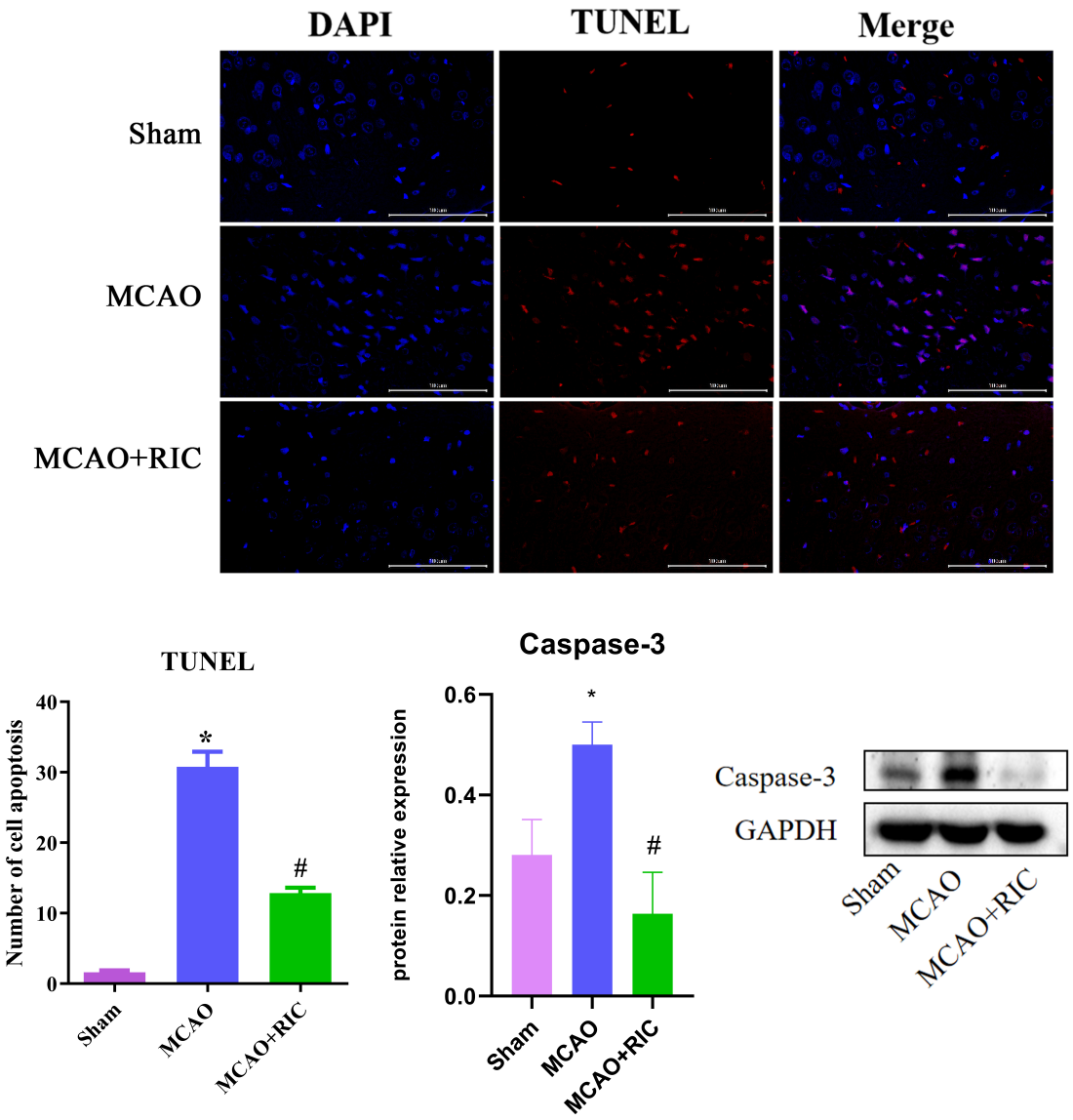

Fig. 6. TUNEL staining and caspase-3 Western blot (WB) (*$p < 0.05$ *vs.* sham; #$p < 0.05$ *vs.* MCAO). TUNEL, Terminal deoxynucleotidyl Utransferase nick-End Labeling. The scale bar = 100 μm.

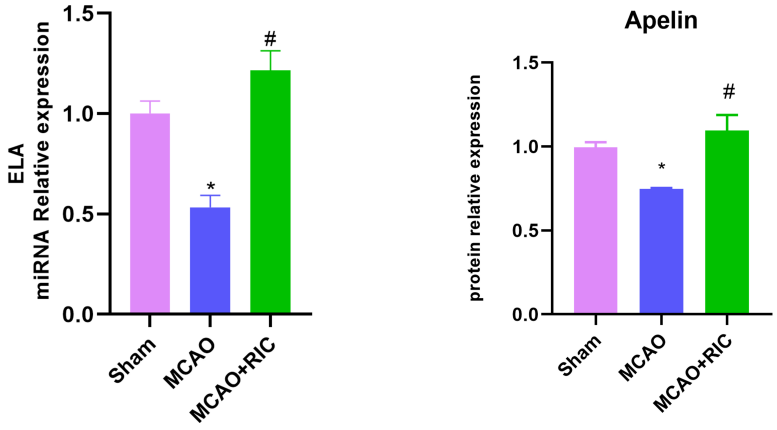

Fig. 7. qPCR for *ELA* and western blot (WB) for apelin (*$p < 0.05$ *vs.* sham; #$p < 0.05$ *vs.* MCAO). qPCR, quantitative polymerase chain reaction.

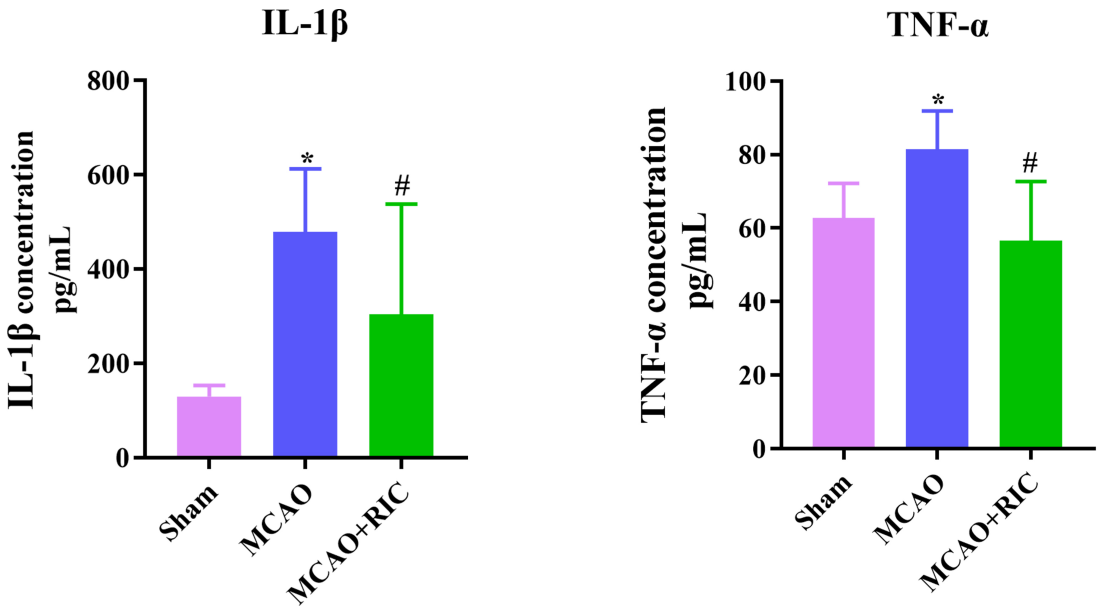

Fig. 8. TNF-α and IL-1β (ELISA) (*$p < 0.05$ *vs.* sham; #$p < 0.05$ *vs.* MCAO). ELISA, enzyme-linked immunosorbent assay.

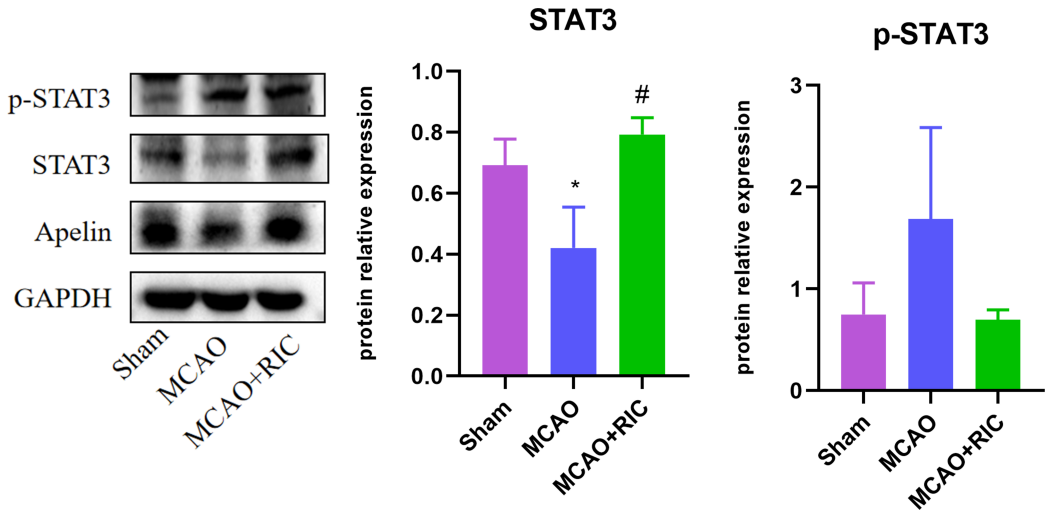

Fig. 9. Apelin, STAT3, and p-STAT3 (WB) (*$p < 0.05$ *vs.* sham; #$p < 0.05$ *vs.* MCAO).

Conversely, the MCAO+RIC group exhibited markedly increased NeuN levels compared to MCAO animals ($p < 0.05$) (Fig. 5).

3.4 After RIC, the Protein Expression of Caspase-3, TNF-α, IL-1β, p-STAT3, HIF-1α, and ATF4 in MCAO Rats Decreased, Whereas the Protein Expression of STAT3, the ELA Gene, and Apelin Increased

Neuronal apoptosis was assessed via caspase-3 expression (TUNEL/WB), while apelin, STAT3, and p-STAT3 protein levels in infarcted tissue were quantified by WB. ELA miRNA expression was measured by qPCR, with HIF-1α and ATF4 detected via immunofluorescence. Proinflammatory cytokines (TNF-α, IL-1β) were analyzed using ELISA. Compared to sham controls, the MCAO group exhibited significantly elevated caspase-3, TNF-α, IL-1β, p-STAT3, HIF-1α, and ATF4 protein levels ($p < 0.05$), but reduced STAT3, ELA, and apelin expression ($p < 0.05$). RIC intervention (MCAO+RIC group) reversed these alterations: expression of caspase-3, TNF-α, IL-1β, p-STAT3, HIF-1α, and ATF4 decreased ($p < 0.05$ *vs.* MCAO), while STAT3, ELA, and apelin were upregulated ($p < 0.05$) (Figs. 6,7,8,9,10). All original WB figures in Fig. 6 and Fig. 9 are provided in the **Supplementary Material**.

3.5 Correlations of the Expression Levels of the ELA and Apelin With Those of Caspase-3 and STAT3

The present study investigated the correlations between ELA miRNA expression/apelin protein expression and Caspase-3/STAT3 expression. The results showed that apelin protein expression was significantly positively

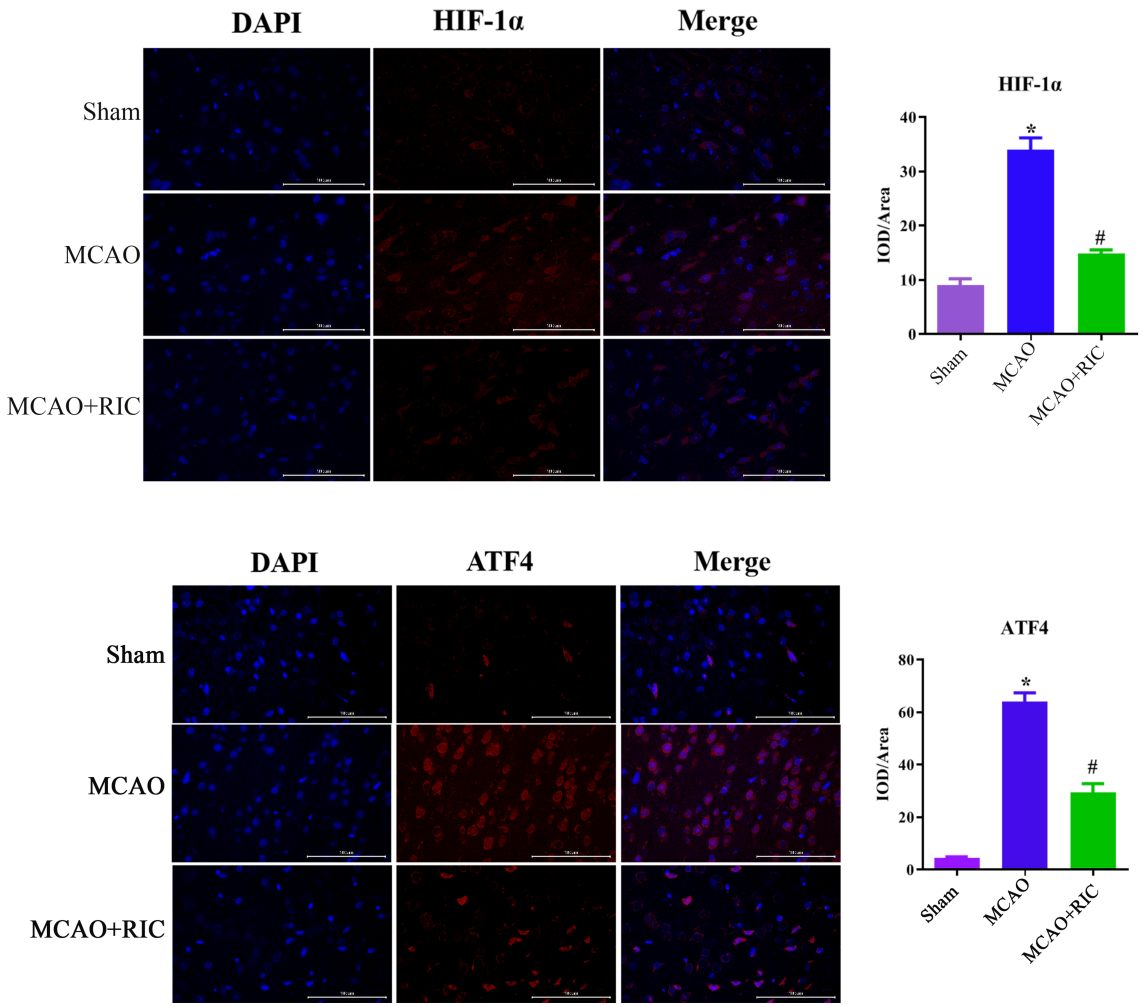

Fig. 10. Immunofluorescence of HIF-1α and ATF4 (*$p < 0.05$ *vs.* sham; #$p < 0.05$ *vs.* MCAO). The scale bar = 100 μm.

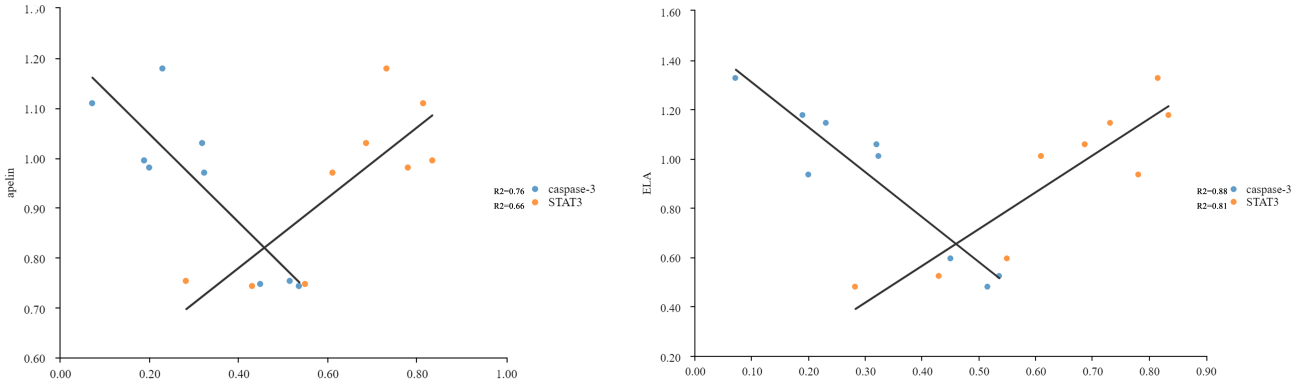

Fig. 11. Correlations between ELA miRNA expression, apelin protein expression and caspase-3 and STAT3 expression.

correlated with STAT3 expression ($R^2 = 0.66$, $p < 0.05$) but negatively correlated with caspase-3 expression ($R^2 = 0.76$, $p < 0.05$). ELA miRNA expression was significantly positively correlated with STAT3 expression ($R^2 = 0.81$, $p < 0.05$) but negatively correlated with caspase-3 expression ($R^2 = 0.88$, $p < 0.05$) (Fig. 11).

4. Discussion

Using MCAO modeling, this study defined the neuroprotective mechanisms of RIC in cerebral ischemia-reperfusion. The findings demonstrated that (1) RIC treatment significantly reduced the cerebral infarct volume and alleviated neuronal damage in

MCAO-induced I/R rats. (2) RIC attenuated the inflammatory response, cellular apoptosis, and reperfusion injury in MCAO-induced I/R rats, possibly through the apelinergic system.

EVT is a therapeutic approach that utilizes endovascular interventional techniques to directly remove thrombi obstructing cerebral arteries, thereby restoring blood flow. Its core objectives are rapid revascularization, reducing disability, and lowering of mortality rates. Clinical-trial data indicated that EVT is safe and effective for anterior circulation stroke patients with low alberta stroke program early CT score (ASPECTS) scores within 6 h of stroke onset [18]. However, successful revascularization does not fully correlate with favorable clinical outcomes, and improving prognoses for patients undergoing endovascular therapy remains a major focus for clinicians [19].

RIC, a low-cost, accessible, safe, noninvasive neuroprotective strategy, has been explored in combination with revascularization therapies. In 2018, Zhao *et al.* [20] demonstrated that RIC application in acute ischemic stroke patients undergoing EVT was safe and feasible. The RIC-CCT study further confirmed that short-term RIC significantly improved cerebral circulation time on the stenotic side, reduced contrast agent extravasation, and decreased the incidence of cerebral hyperperfusion syndrome after carotid artery stenting in patients with severe internal carotid artery stenosis [7]. Nevertheless, the neuroprotective mechanisms of RIC in revascularization therapy have remained unclear. The present study aimed to investigate the neuroprotective mechanisms of RIC during ischemia-reperfusion using an MCAO ischemia-reperfusion model. To align with clinical practice, RIC treatment was administered post-reperfusion in MCAO rats.

Previous randomized controlled trials have demonstrated that pharmacotherapy combined with RIC, administered after acute cerebral infarction, can reduce cerebral infarct volume, improve functional outcomes, prevent stroke recurrence, and attenuate cognitive impairment [21]. In MCAO animal models, RIC has been shown to mitigate infarct size and ameliorate neurological deficits [22,23], which is consistent with the findings of our present study.

The pathophysiology of ischemic brain injury involves the activation of detrimental signaling cascades, including hypoxia, endoplasmic reticulum stress, glucose deprivation, inflammatory responses, and apoptotic pathways [24]. A study has suggested that the ELA-apelin-APJ system is implicated in ischemic stroke, critically protecting against ischemia-induced apoptosis and neurological deficits, highlighting its therapeutic potential [25]. Research has demonstrated that apelin-13 protects against oxidative damage in ischemic stroke via the AMP-activated protein kinase/glycogen synthase kinase-3 beta/nuclear factor erythroid 2-related factor 2 (AMPK/GSK-3β/Nrf2) pathway [26]. Additionally, different apelin isoforms inhibit neuronal apoptosis through distinct mechanisms [27,28]. In rat models, apelin also modulates inflammatory responses by suppressing proinflammatory mediators including IL-1β, TNF-α, and intercellular adhesion molecule 1 (ICAM-1) [29]. Notably, RIC shares neuroprotective mechanisms with the ELA-apelin-APJ system, as RIC mitigates neuronal injury via anti-apoptotic, anti-inflammatory, and antioxidant pathways [30]. These findings led us to hypothesize that RIC alleviates inflammation, apoptosis, and reperfusion injury in MCAO rats by modulating the apelinergic system.

The relationship between RIC and the ELA-apelin-APJ system in the field of ischemic stroke remains unexplored. A previous study has demonstrated that in renal I/R injury models, RIC can mitigate ischemia-induced renal damage by modulating apelin expression [31]. Our research has demonstrated that in the MCAO model, after treatment with RIC, the expression of apelin and ELA is increased, the volume of cerebral infarction is reduced, and neuronal damage is alleviated. This indicates that RIC can alleviate brain injury caused by ischemia by regulating the expression of apelin and ELA. Our results further demonstrated that in the MCAO+RIC group, RIC significantly upregulated STAT3 and ELA expression, along with apelin levels, while concurrently downregulating the expression of caspase-3, TNF-α, IL-1β, phosphorylated STAT3 (p-STAT3), HIF-1α, and ATF4. These molecular alterations exhibited significant linear correlations. Collectively, these data indicated that RIC ameliorates neuronal injury and attenuates apoptosis and neuroinflammation through coordinated mechanisms, including the correction of ischemic hypoxia (reflected by HIF-1α reduction), alleviation of endoplasmic reticulum stress (indicated by ATF4 decrease), and suppression of the inflammatory response (evidenced by diminished p-STAT3, TNF-α, and IL-1β). It is important to note that our findings suggest that the ELA-apelin-APJ system serves as a key upstream mediator of these multifaceted neuroprotective effects conferred by RIC.

A key limitation of this study is the absence of pharmacological interventions using activators or inhibitors targeting the ELA-apelin-APJ system. This finding precludes definitive conclusions regarding whether RIC alleviates neuronal apoptosis and inflammation in the MCAO-induced ischemia-reperfusion model via a specific pathway or through synergistic interactions of multiple mechanisms. Future studies will incorporate these tools to dissect the precise contributions of individual signaling components within the ELA-apelin-APJ axis and clarify the mechanistic hierarchy underlying RIC-mediated neuroprotection.

5. Conclusion

The focus of the present study was to explore the neuroprotective effects of RIC and the possible mechanisms underlying its effect after reperfusion injury in ischemic stroke. These findings support the hypothesis that RIC alleviates neuronal apoptosis and inflammation in an MCAO-induced ischemia/reperfusion model by modulating the ELA-apelin-APJ system. These findings suggest that the mechanism by which RIC alleviates ischemic stroke may involve the modulation of the ELA-apelin-APJ system.

Abbreviations

RIC, Remote ischemic conditioning; MCAO, middle cerebral artery occlusion; WB, Western blotting; HE, Hematoxylin-eosin; LVO, large vessel occlusion; EVT, Endovascular thrombectomy; HIF-1α, hypoxia-inducible factor 1α; STAT3, signal transducer and activator of transcription 3; ATF4, activating transcription factor 4; HREs, hypoxia-response elements; I/R, ischemia-reperfusion; SD, Sprague-Dawley; SPF, specific-pathogen-free; NDSs, neurological deficit scores; IL-1β, interleukin-1β; RCTs, randomized controlled trials; ER, endoplasmic reticulum.

Availability of Data and Materials

The data that support the findings of this study are available in the supplementary material of this article.

Author Contributions

JS: Conceptualization, Methodology, Validation, Formal analysis, Investigation, Data curation, Writing—review and editing, Supervision, Project administration. FZ: Conceptualization, Methodology, Validation, Formal analysis, Data curation, Resources, Writing—review and editing, Supervision, Project administration, Funding acquisition. YW: Conceptualization, Methodology, Validation, Formal analysis, Investigation, Data curation, Writing—original draft, Writing—review and editing, Visualization. XC: Validation, Formal analysis, Investigation, Data curation. ZP: Validation, Formal analysis, Investigation. XW: Validation, Formal analysis, Investigation. SG: Validation, Formal analysis, Investigation. CS: Validation, Formal analysis, Investigation. JR: Data curation. All authors contributed to critical revision of the manuscript for important intellectual content. All authors read and approved the final manuscript. All authors have participated sufficiently in the work and agreed to be accountable for all aspects of the work.

Ethics Approval and Consent to Participate

All animal experiments received approval from the Institutional Animal Care and Use Committee of Jiangxi Zhonghong Boyuan Biotechnology Co., Ltd. (approval number: LL-202403080006) and conducted in compliance with China's national laboratory animal regulations: the Regulations on the Administration of Laboratory Animals (State Science and Technology Commission) and Implementation Rules for Medical Laboratory Animal Administration (Ministry of Health). Experimental procedures strictly adhered to the ARRIVE reporting guidelines.

Acknowledgment

Not applicable.

Funding

This study was supported by the Taiyuan Bureau of Science and Technology, Science, Technology, and Innovation Program of the National Regional Medical Center (No. 202227).

Conflict of Interest

The authors declare no conflict of interest.

Supplementary Material

Supplementary material associated with this article can be found, in the online version, at https://doi.org/10.31083/JIN39897.

References

[1] GBD 2019 Stroke Collaborators. Global, regional, and national burden of stroke and its risk factors, 1990-2019: a systematic analysis for the Global Burden of Disease Study 2019. The Lancet. Neurology. 2021; 20: 795–820. https://doi.org/10.1016/S1474-4422(21)00252-0.

[2] de Havenon A, Zaidat OO, Amin-Hanjani S, Nguyen TN, Bangad A, Abbasi M, *et al*. Large Vessel Occlusion Stroke due to Intracranial Atherosclerotic Disease: Identification, Medical and Interventional Treatment, and Outcomes. Stroke. 2023; 54: 1695–1705. https://doi.org/10.1161/STROKEAHA.122.040008.

[3] Nie X, Leng X, Miao Z, Fisher M, Liu L. Clinically Ineffective Reperfusion After Endovascular Therapy in Acute Ischemic Stroke. Stroke. 2023; 54: 873–881. https://doi.org/10.1161/STROKEAHA.122.038466.

[4] Jovin TG, Nogueira RG, Lansberg MG, Demchuk AM, Martins SO, Mocco J, *et al*. Thrombectomy for anterior circulation stroke beyond 6 h from time last known well (AURORA): a systematic review and individual patient data meta-analysis. Lancet. 2022; 399: 249–258. https://doi.org/10.1016/S0140-6736(21)01341-6.

[5] Kan X, Yan Z, Wang F, Tao X, Xue T, Chen Z, *et al*. Efficacy and safety of remote ischemic conditioning for acute ischemic stroke: A comprehensive meta-analysis from randomized controlled trials. CNS Neuroscience & Therapeutics. 2023; 29: 2445–2456. https://doi.org/10.1111/cns.14240.

[6] Sharma D, Maslov LN, Singh N, Jaggi AS. Remote ischemic preconditioning-induced neuroprotection in cerebral ischemia-reperfusion injury: Preclinical evidence and mechanisms. European Journal of Pharmacology. 2020; 883: 173380. https://doi.org/10.1016/j.ejphar.2020.173380.

[7] Liu QY, Cui Y, Li W, Qiu J, Nguyen TN, Chen HS. Effect of remote ischemic preconditioning on cerebral circulation time in severe carotid artery stenosis: Results from the RIC-CCT trial. Cell Reports. Medicine. 2024; 5: 101796. https://doi.org/10.1016/j.xcrm.2024.101796.

[8] Respekta N, Pich K, Dawid M, Mlyczyńska E, Kurowska P, Rak A. The Apelinergic System: Apelin, ELABELA, and APJ Action on Cell Apoptosis: Anti-Apoptotic or Pro-Apoptotic Effect? Cells. 2022; 12: 150. https://doi.org/10.3390/cells12010150.

[9] He L, Xu J, Chen L, Li L. Apelin/APJ signaling in hypoxia-related diseases. Clinica Chimica Acta; International Journal of Clinical Chemistry. 2015; 451: 191–198. https://doi.org/10.1016/j.cca.2015.09.029.

[10] Han S, Wang G, Qi X, Englander EW, Greeley GH, Jr. Involvement of a Stat3 binding site in inflammation-induced enteric apelin expression. American Journal of Physiology. Gastrointestinal and Liver Physiology. 2008; 295: G1068–G1078. https://doi.org/10.1152/ajpgi.90493.2008.

[11] Jeong K, Oh Y, Kim SJ, Kim H, Park KC, Kim SS, *et al*. Apelin is transcriptionally regulated by ER stress-induced ATF4 expression via a p38 MAPK-dependent pathway. Apoptosis: an International Journal on Programmed Cell Death. 2014; 19: 1399–1410. https://doi.org/10.1007/s10495-014-1013-0.

[12] Shan Y, Wang L, Sun J, Chang S, Di W, Lv H. Exercise preconditioning attenuates cerebral ischemia-induced neuronal apoptosis, Th17/Treg imbalance, and inflammation in rats by inhibiting the JAK2/STAT3 pathway. Brain and Behavior. 2023; 13: e3030. https://doi.org/10.1002/brb3.3030.

[13] Wu Y, Wang X, Zhou X, Cheng B, Li G, Bai B. Temporal Expression of Apelin/Apelin Receptor in Ischemic Stroke and its Therapeutic Potential. Frontiers in Molecular Neuroscience. 2017; 10: 1. https://doi.org/10.3389/fnmol.2017.00001.

[14] Chen D, Lee J, Gu X, Wei L, Yu SP. Intranasal Delivery of Apelin-13 Is Neuroprotective and Promotes Angiogenesis After Ischemic Stroke in Mice. ASN Neuro. 2015; 7: 1759091415605114. https://doi.org/10.1177/1759091415605114.

[15] Xu P, Kong L, Tao C, Zhu Y, Cheng J, Li W, *et al*. Elabela-APJ axis attenuates cerebral ischemia/reperfusion injury by inhibiting neuronal ferroptosis. Free Radical Biology & Medicine. 2023; 196: 171–186. https://doi.org/10.1016/j.freeradbiomed.2023.01.008.

[16] Zhang KL, Li SM, Hou JY, Hong YH, Chen XX, Zhou CQ, *et al*. Elabela, a Novel Peptide, Exerts Neuroprotective Effects Against Ischemic Stroke Through the APJ/miR-124-3p/CTDSP1/AKT Pathway. Cellular and Molecular Neurobiology. 2023; 43: 2989–3003. https://doi.org/10.1007/s10571-023-01352-6.

[17] Li W, Xu P, Kong L, Feng S, Shen N, Huang H, *et al*. Elabela-APJ axis mediates angiogenesis via YAP/TAZ pathway in cerebral ischemia/reperfusion injury. Translational Research: the Journal of Laboratory and Clinical Medicine. 2023; 257: 78–92. https://doi.org/10.1016/j.trsl.2023.02.002.

[18] Chen H, Lee JS, Michel P, Yan B, Chaturvedi S. Endovascular Stroke Thrombectomy for Patients With Large Ischemic Core: A Review. JAMA Neurology. 2024; 81: 1085–1093. https://doi.org/10.1001/jamaneurol.2024.2500.

[19] Wassélius J, Arnberg F, von Euler M, Wester P, Ullberg T. Endovascular thrombectomy for acute ischemic stroke. Journal of Internal Medicine. 2022; 291: 303–316. https://doi.org/10.1111/joim.13425.

[20] Zhao W, Che R, Li S, Ren C, Li C, Wu C, *et al*. Remote ischemic conditioning for acute stroke patients treated with thrombectomy. Annals of Clinical and Translational Neurology. 2018; 5: 850–856. https://doi.org/10.1002/acn3.588.

[21] Li Q, Guo J, Chen HS, Blauenfeldt RA, Hess DC, Pico F, *et al*. Remote Ischemic Conditioning With Medical Management or Reperfusion Therapy for Acute Ischemic Stroke: A Systematic Review and Meta-Analysis. Neurology. 2024; 102: e207983. https://doi.org/10.1212/WNL.0000000000207983.

[22] Li S, Yang Y, Li N, Li H, Xu J, Zhao W, *et al*. Limb Remote Ischemic Conditioning Promotes Neurogenesis after Cerebral Ischemia by Modulating miR-449b/Notch1 Pathway in Mice. Biomolecules. 2022; 12: 1137. https://doi.org/10.3390/biom12081137.

[23] Sun YY, Zhu HJ, Zhao RY, Zhou SY, Wang MQ, Yang Y, *et al*. Remote ischemic conditioning attenuates oxidative stress and inflammation via the Nrf2/HO-1 pathway in MCAO mice. Redox Biology. 2023; 66: 102852. https://doi.org/10.1016/j.redox.2023.102852.

[24] Paul S, Candelario-Jalil E. Emerging neuroprotective strategies for the treatment of ischemic stroke: An overview of clinical and preclinical studies. Experimental Neurology. 2021; 335: 113518. https://doi.org/10.1016/j.expneurol.2020.113518.

[25] Li A, Zhao Q, Chen L, Li Z. Apelin/APJ system: an emerging therapeutic target for neurological diseases. Molecular Biology Reports. 2023; 50: 1639–1653. https://doi.org/10.1007/s11033-022-08075-9.

[26] Duan J, Cui J, Yang Z, Guo C, Cao J, Xi M, *et al*. Neuroprotective effect of Apelin 13 on ischemic stroke by activating AMPK/GSK-3β/Nrf2 signaling. Journal of Neuroinflammation. 2019; 16: 24. https://doi.org/10.1186/s12974-019-1406-7.

[27] Zeng XJ, Yu SP, Zhang L, Wei L. Neuroprotective effect of the endogenous neural peptide apelin in cultured mouse cortical neurons. Experimental Cell Research. 2010; 316: 1773–1783. https://doi.org/10.1016/j.yexcr.2010.02.005.

[28] Gu Q, Zhai L, Feng X, Chen J, Miao Z, Ren L, *et al*. Apelin-36, a potent peptide, protects against ischemic brain injury by activating the PI3K/Akt pathway. Neurochemistry International. 2013; 63: 535–540. https://doi.org/10.1016/j.neuint.2013.09.017.

[29] Soliman M, Arafah M. Apelin protect against multiple organ injury following hemorrhagic shock and decrease the inflammatory response. International Journal of Applied & Basic Medical Research. 2015; 5: 195–199. https://doi.org/10.4103/2229-516X.165377.

[30] Baranova K, Nalivaeva N, Rybnikova E. Neuroadaptive Biochemical Mechanisms of Remote Ischemic Conditioning. International Journal of Molecular Sciences. 2023; 24: 17032. https://doi.org/10.3390/ijms242317032.

[31] Gholampour F, Bagheri A, Barati A, Masoudi R, Owji SM. Remote Ischemic Perconditioning Modulates Apelin Expression After Renal Ischemia-Reperfusion Injury. The Journal of Surgical Research. 2020; 247: 429–437. https://doi.org/10.1016/j.jss.2019.09.063.